



## Electrochemical Performance of $\text{Na}_2\text{Mn}_3\text{O}_7$ as a Cathode Material in Sodium-Ion Batteries Using the Precipitation Method with Ethylene Glycol Chelating Agent

Achmad Subhan<sup>1</sup>, Muhammad Thariq As Sulaiman<sup>2</sup>, and Syahrul Humaidi<sup>2\*</sup>

<sup>1</sup>National Research and Innovation Agency (BRIN), South Tangerang 15314, Indonesia

<sup>2</sup>Department of Physics, Faculty of Mathematics and Natural Science, Universitas Sumatera Utara, 20155, Indonesia

\*Corresponding Author: [syahrull@usu.ac.id](mailto:syahrull@usu.ac.id)

### ARTICLE INFO

#### Article history:

Received 2 October 2023  
Revised 12 February 2024  
Accepted 19 February 2024  
Available online 29 February 2024

E-ISSN: 2656-0755

P-ISSN: 2656-0747

#### How to cite:

A. Subhan, M. T. A. Sulaiman, and S. Humaidi, "Electrochemical Performance of  $\text{Na}_2\text{Mn}_3\text{O}_7$  as a Cathode Material in Sodium-Ion Batteries Using the Precipitation Method with Ethylene Glycol Chelating Agent," Journal of Technomaterial Physics, vol. 06, no. 01, pp. 15-20, Feb. 2024, doi: 10.32734/jotpp.v6i1.13867.

### ABSTRACT

Tests were conducted on  $\text{Na}_2\text{Mn}_3\text{O}_7$  as a cathode material in sodium-ion batteries, aiming to synthesize  $\text{Na}_2\text{Mn}_3\text{O}_7$  precursor using commercial and synthetic  $\text{MnCO}_3$  variants. Sample A utilized commercial  $\text{MnCO}_3$ , while sample B utilized  $\text{MnCO}_3$  synthesized from  $\text{MnSO}_4 \cdot \text{H}_2\text{O}$  and  $\text{Na}_2\text{CO}_3$ . Both variants were mixed with  $\text{Na}_2\text{CO}_3$  to form  $\text{Na}_2\text{Mn}_3\text{O}_7$  precursor, which was then sintered at  $700^\circ\text{C}$  for 4 hours, ground, and sieved. A slurry was prepared by mixing the active materials PVDF: Super P in an 8:1:1 ratio with 3.5 mL of NMP. Sample A exhibited a conductivity of  $3.4706 \times 10^{-7}$  S/cm, and sample B had a conductivity of  $2.7304 \times 10^{-7}$  S/cm in the EIS results. In the CV test, sample A showed oxidation and reduction peaks at 2.77 V and 1.62 V, respectively, while sample B had peaks at 2.842 V and 1.716 V. In the CD test, sample A reached maximum and minimum peaks of 4.3 V and 1.4 V, while sample B reached peaks of 4.2 V and 1.3 V. Sample A exhibited a capacity of 117.02 mAh/g on charge and 93.47 mAh/g on discharge, whereas sample B showed capacities of 79.17 mAh/g on charge and 65.79 mAh/g on discharge. These results indicate the superior performance of sample A over sample B.

**Keywords:** Composite Board, Corn Husk Fiber, Epoxy, Sawdust, Water Hyacinth Fiber

### ABSTRAK

Tes dilakukan pada  $\text{Na}_2\text{Mn}_3\text{O}_7$  sebagai bahan katoda dalam baterai ion natrium, dengan tujuan menyintesis prekursor  $\text{Na}_2\text{Mn}_3\text{O}_7$  menggunakan varian  $\text{MnCO}_3$  komersial dan sintesis. Sampel A menggunakan  $\text{MnCO}_3$  komersial, sedangkan sampel B menggunakan  $\text{MnCO}_3$  yang disintesis dari  $\text{MnSO}_4 \cdot \text{H}_2\text{O}$  dan  $\text{Na}_2\text{CO}_3$ . Kedua varian dicampur dengan  $\text{Na}_2\text{CO}_3$  untuk membentuk prekursor  $\text{Na}_2\text{Mn}_3\text{O}_7$ , yang kemudian disinter pada suhu  $700^\circ\text{C}$  selama 4 jam, digiling, dan disaring. Slurry disiapkan dengan mencampur bahan aktif PVDF: Super P dalam rasio 8:1:1 dengan 3,5 mL NMP. Sampel A menunjukkan konduktivitas sebesar  $3,4706 \times 10^{-7}$  S/cm, dan sampel B memiliki konduktivitas sebesar  $2,7304 \times 10^{-7}$  S/cm dalam hasil EIS. Pada uji CV, sampel A menunjukkan puncak oksidasi dan reduksi pada 2,77 V dan 1,62 V, sementara sampel B memiliki puncak pada 2,842 V dan 1,716 V. Pada uji CD sampel A mencapai puncak maksimum dan minimum sebesar 4,3 V dan 1,4 V, sementara sampel B mencapai puncak pada 4,2 V dan 1,3 V. Sampel A menunjukkan kapasitas sebesar 117,02 mAh/g pada pengisian dan 93,47 mAh/g pada pengosongan muatan, sedangkan sampel B menunjukkan kapasitas sebesar 79,17 mAh/g pada pengisian dan 65,79 mAh/g pada pengosongan muatan. Hasil ini menunjukkan performa yang lebih unggul dari sampel A dibandingkan dengan sampel B.

**Kata kunci:** Epoksi, Papan Komposit, Serat Eceng Gondok, Serat Kulit Jagung, Serbuk Gergaji



This work is licensed under a Creative Commons Attribution-ShareAlike 4.0 International.

<http://doi.org/10.32734/jotpp.v6i1.13867>

## 1. Introduction

The Indonesian government targets that in 2020, it will bring 13 million electric vehicles, and in 2030 it will reach 100 million. Electric vehicles do not have emissions or exhaust gases like conventional vehicles today [1]. Lithium-ion batteries (LIBs) are the most commercially viable energy storage devices due to their energy density, long lifespan, safety, low pollution, and affordability [2]. However, limited lithium resources have led to an increase in its price, thus limiting its applications [3].

The oxide structure based on the transition metal manganese (Na-Mn-O) is of interest to study because it is environmentally friendly, inexpensive, and has a high capacity [4]. Recently, after its initial discovery, the Na-Mn-O structure was re-evaluated with Triclinic  $\text{Na}_2\text{Mn}_3\text{O}_7$  combined unit cell lattice parameters. Sodium manganese oxide ( $\text{Na}_2\text{Mn}_3\text{O}_7$ ) is intriguing because it can be charged at 4.7 V with a capacity of approximately  $117 \text{ mAh.g}^{-1}$ , thereby supporting the development of cathodes in SIB devices [5].

Batteries serve as an energy source by converting chemical energy into electrical energy, powering commonly used devices such as cell phones, computers, and vehicles [6]. Selecting the appropriate electrode material is crucial for developing and researching SIBs [7]. Despite having different charge transfer mechanisms, sodium-ion batteries (SIB) and LIBs share similar battery components and energy storage mechanisms [8]. Recently, with the emergence of the energy storage market, room-temperature SIBs have regained research interest due to their abundance and affordability [9]. The primary challenge for SIBs is finding suitable electrode materials with good sodium storage capacity, as their electrochemical properties determine specific capacitance and operating voltage [10].

However, this strategy is not always applicable due to clear differences in the intercalation behavior of Na and Li [11]. Factors influencing the feasibility and reaction rate of solids include reaction conditions, structural properties of reactants, surface area of solids, reactivity, and thermodynamic free energy changes associated with the reaction [12]. The precipitation process has been recently modified and developed to improve LIB/SIB properties, such as larger surface area, better microstructure, and effective calcination temperature. Modifications include the use of chelating agents [13]. The chelating agents utilized include sugars and ethylene glycol [14].

Chelating agents are among the additives that influence LIB/SIB synthesis, as they contribute to good cationic distribution and the formation of homogeneous crystal particles [15]. Additionally, chelating agents play a crucial role in the preparation of nano powders at low temperatures [16]. This method allows nanosized particles to synthesize, enhancing surface area [17]. The formation of  $\text{Na}_2\text{Mn}_3\text{O}_7$  involves mixing MnO powder synthesized using the solid method with  $\text{Na}_2\text{CO}_3$  precursor, followed by calcination at a temperature of  $800^\circ\text{C}$  in an oxidizing atmosphere for 1 hour. In 2015, it was discovered that graphite can store sodium through solvent intercalation in an ether-based electrolyte. Hence, it is imperative to delve into the comparison between the synthesized  $\text{Na}_2\text{Mn}_3\text{O}_7$  precursor using commercial and synthetic  $\text{MnCO}_3$  variants.

## 2. Method

This research underwent three stages: (i) synthesizing sodium manganese oxide ( $\text{Na}_2\text{Mn}_3\text{O}_7$ ) from two different sources: commercial  $\text{MnCO}_3$  and synthesized  $\text{MnCO}_3$ , (ii) coin cell assembly, and (iii) characterization using electrochemical impedance spectroscopy (EIS) to determine conductivity values, cyclic voltammetry find redox information, and charge-discharge to determine battery capacity for electrochemical testing. The number of  $\text{Na}_2\text{Mn}_3\text{O}_7$  samples in this study was two samples.

### 2.1. Synthesis of Sodium Manganese Oxide ( $\text{Na}_2\text{Mn}_3\text{O}_7$ )

At the beginning of this research,  $\text{Na}_2\text{Mn}_3\text{O}_7$  was synthesized using the precipitation method with a variety of sources from commercial  $\text{MnCO}_3$  and synthesized  $\text{MnCO}_3$ .

#### 2.1.1. Synthesis of $\text{Na}_2\text{Mn}_3\text{O}_7$ from Commercial $\text{MnCO}_3$

In the first sample, commercial  $\text{MnCO}_3$  weighed 10.7073 grams, and 3.5004 grams of  $\text{Na}_2\text{CO}_3$  were added. Then, both ingredients were crushed using a mortar until homogeneous. Then, the mixed ingredients were dissolved in 20 mL DI water mixed with 10mL ethanol and ethylene glycol (30% of DI water + ethanol). Then, it was dried using a hotplate while stirring using a magnetic stirrer until thickened for 2 hours. Then, it was put in the oven for 20 hours at a temperature of  $80^\circ\text{C}$ . The dry ingredients were then removed from the oven. After that, the material was sintered in a furnace at a temperature of  $700^\circ\text{C}$  for 4 hours [5]. The sample was coded sample A.

### 2.1.2. Synthesis of $\text{Na}_2\text{Mn}_3\text{O}_7$ from synthesized $\text{MnCO}_3$

In the second sample, 6.76 grams of  $\text{MnSO}_4 \cdot 1\text{H}_2\text{O}$  were prepared and dissolved in 40 mL of distilled water. Next, it was mixed with 4.24 grams of  $\text{Na}_2\text{CO}_3$  dissolved in 40 mL of distilled water using a hotplate and magnetic stirrer for 2 hours. The mixed solution will form a cream-colored  $\text{MnCO}_3$  gel. After complete mixing, 500 mL of distilled water was added to the solution so that the pH of the solution became neutral. Next, the sample was allowed to settle, causing the sediment to separate from the water. Subsequently, the separated water was drained off. The sample was then placed in an oven at  $80^\circ\text{C}$  for 20 hours to dry. Once dried, the  $\text{MnCO}_3$  material was combined with 1.311 grams of  $\text{Na}_2\text{CO}_3$  and thoroughly mixed until homogeneous. This mixture was sintered in a furnace at  $700^\circ\text{C}$  for 4 hours [5]. The resulting sample is designated as sample B.

### 2.2. Battery Cell Sample Preparation

The sintered results are initially crushed with a mortar and subsequently sieved through a 400-mesh sieve. The sieved material is then weighed using an analytical balance.  $\text{Na}_2\text{Mn}_3\text{O}_7$  powder is blended with PVDF Super P at a ratio of 80%:10%:10%. Following this, 3.5 mL of NMP is added to the mixture. Stir the ingredients thoroughly until they form a slurry.

### 2.3. Electrochemical Testing of Sodium Manganese Oxide ( $\text{Na}_2\text{Mn}_3\text{O}_7$ )

The testing of battery cell samples involves three main tests:

- Electrochemical impedance spectrometry (EIS) test utilizes an inductance, capacitance, and resistance (LCR) meter to measure the inductance, capacitance, and resistance of the sample.
- Cyclic Voltammetry (CV) testing: This test is employed to assess the battery performance and identify reduction and oxidation peaks occurring during the electrochemical cycle of the sample battery cells. AutoLab PGSTAT equipment is used for this purpose.
- The charge-discharge (CD) test involves battery and discharge testing conducted using AutoLab PGSTAT equipment.

## 3. Result and Discussion

### 3.1. Electrochemical Impedance Spectroscopy (EIS) Analysis

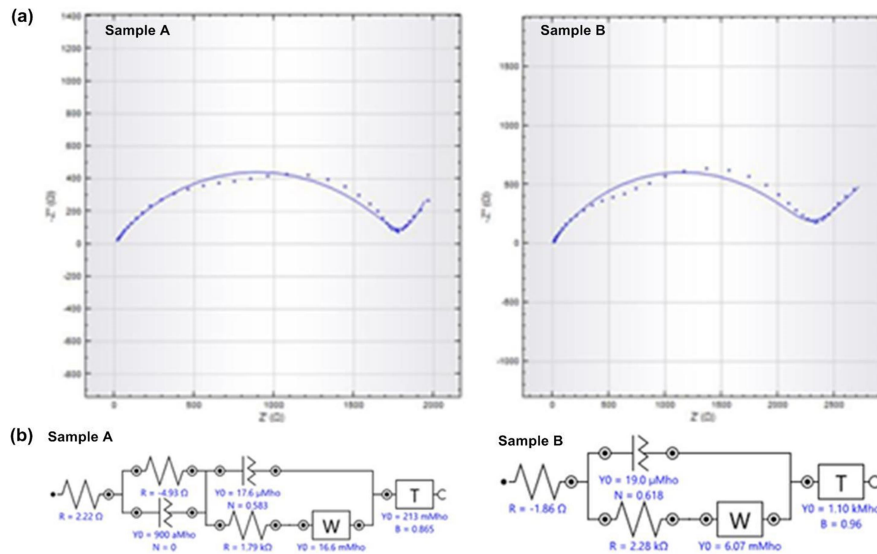


Figure 1. (a) Nyquist plot of samples A and B, and (b) Circuit of samples A and B.

Table 1. Electrochemical Impedance Spectroscopy (EIS) results of sample A and B.

Sample	$R_s(\Omega)$	$R_{ct}(\Omega)$	$R_{tot}(\Omega)$	Conductivity( $\sigma$ )(S/cm)
A	2.22	1.79	1,792.22	$3.4706 \times 10^{-7}$
B	-1.86	2.28	2,278.14	$2.7304 \times 10^{-7}$

Drawing from Figure 1 and Table 1, a comparison between samples A and B reveals differences in conductivity values and graph representations. Sample A exhibits a conductivity value of  $3.4706 \times 10^{-7}$  S/cm, greater than sample B's ( $2.7304 \times 10^{-7}$  S/cm). Consequently, it can be inferred that sample A boasts superior diffusion and conductivity compared to sample B.

### 3.2. Cyclic Voltammetry (CV) Analysis

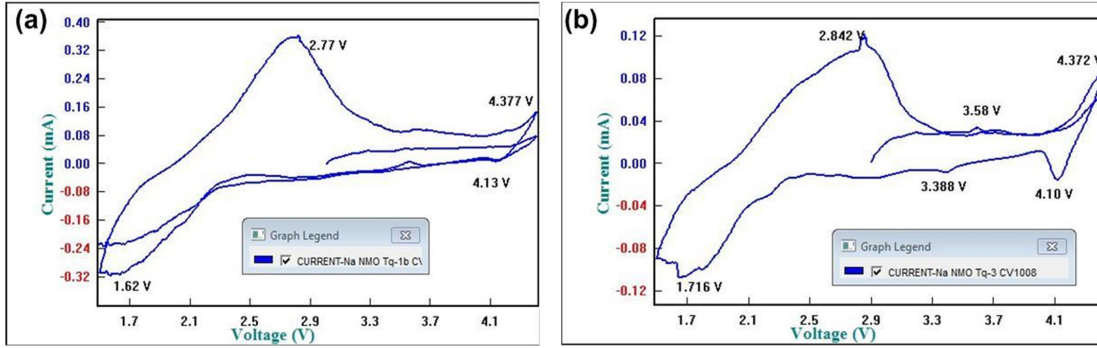


Figure 2. CV curve of (a) Sample A and (b) Sample B.

Table 2. Electrochemical Impedance Spectroscopy (EIS) results of sample A and B.

Sample	Oxidation Peak (V)	Reduction Peak (V)
A	2.77	1.62
B	2.84	1.72

Upon examining Figure 2 and Table 2, it is evident that in sample A, the oxidation peak is observed at 2.77 V, while the reduction peak occurs at 1.62 V. Conversely, in sample B, the oxidation peak is recorded at 2.84 V, with the reduction peak observed at 1.72 V. Despite minor variations, the CV test results for samples A and B indicate closely aligned values, suggesting negligible differences between them. Both samples demonstrate successful redox processes, rendering them suitable for use as battery cells, which will subsequently undergo charge-discharge (CD) testing.

### 3.3. Charge Discharge (CD) Analysis

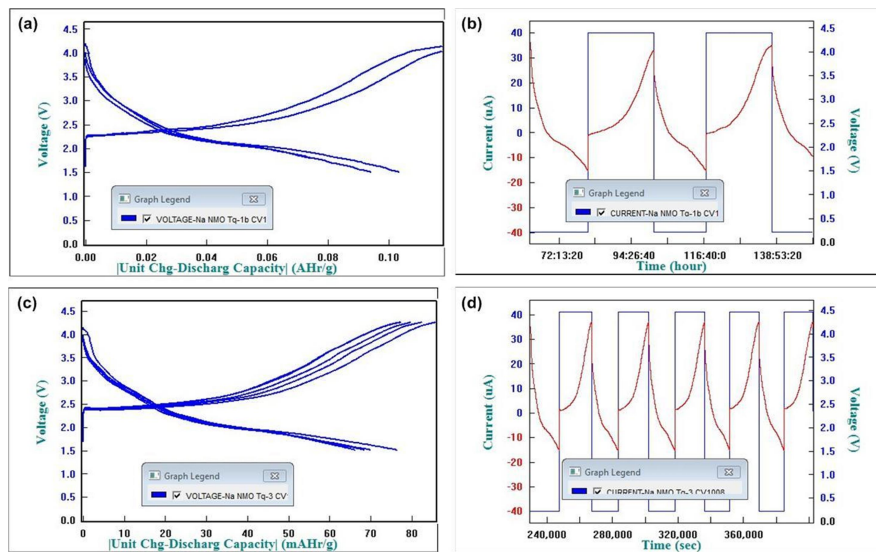


Figure 3. (a) CD test results for sample A, (b) CD test results of occurrence process of 3 cycles for sample A, (c) CD test results for sample B, and (d) CD test results of occurrence process of 5 cycles for sample B.

Based on Figure 3, sample A reached a maximum peak of 4.3 V and then dipped to its lowest point of 1.4 V, while sample B achieved a maximum peak of 4.2 V with a lowest point of 1.3 V. In terms of capacity, sample A exhibited 117.02 mAh/g during charging and 93.47 mAh/g during discharging, whereas sample B showed a capacity of 79.17 mAh/g during charging and 65.79 mAh/g during discharging. The observed low capacity can be attributed to various factors, including incomplete  $\text{Na}_2\text{Mn}_3\text{O}_7$  synthesis, imperfect phase formation, and structural damage, leading to results that deviate from expectations and hinder the accommodation of larger capacity loads. Differences in temperature and time during sintering may also impact the resulting electrochemical performance.

#### 4. Conclusion

Testing the EIS, CV, and CD performance of the  $\text{Na}_2\text{Mn}_3\text{O}_7$  cathode material from both samples yielded promising results. Sample A exhibited a conductivity of  $3.4706 \times 10^{-7}$  S/cm, while sample B showed a slightly lower conductivity of  $2.7304 \times 10^{-7}$  S/cm. In the CV test, sample A displayed oxidation and reduction peaks at 2.77 V and 1.62 V, respectively, whereas sample B showed peaks at 2.842 V and 1.716 V. During the CD test, sample A reached a maximum voltage of 4.3 V and a minimum of 1.4 V, outperforming sample B which reached 4.2 V and 1.3 V respectively. Sample A also demonstrated higher capacities of 117.02 mAh/g during charging and 93.47 mAh/g during discharging, compared to sample B, with capacities of 79.17 mAh/g during charging and 65.79 mAh/g during discharging. However, both samples exhibited lower-than-expected capacities, likely due to incomplete synthesis of  $\text{Na}_2\text{Mn}_3\text{O}_7$ , imperfect phase formation, and structural damage. Additionally, sintering temperature and time variations may have affected the electrochemical performance.

#### References

- [1] T. P. Cahyono, T. Hardianto, and B. S. Kaloko, "Pengujian Karakteristik Baterai Lithium-Ion Dengan Metode Fuzzy Dengan Beban Bervariasi," *J. Arus Elektro Indones.*, vol. 6, no. 3, p. 82, 2020, doi: 10.19184/jaei.v6i3.19708.
- [2] M. M. Gaikwad, M. Kakunuri, and C. S. Sharma, "Enhanced catalytic graphitization of resorcinol formaldehyde derived carbon xerogel to improve its anodic performance for lithium ion battery," *Mater. Today Commun.*, vol. 20, p. 100569, 2019, doi: 10.1016/j.mtcomm.2019.100569.
- [3] K. Shiprath, H. Manjunatha, K. C. Babu Naidu, A. Khan, A. M. Asiri, and R. Boddula, " $\text{Na}_3\text{MnPO}_4\text{CO}_3$  as cathode for aqueous sodium ion batteries: Synthesis and electrochemical characterization," *Mater. Chem. Phys.*, vol. 248, no. November 2019, p. 122952, 2020, doi: 10.1016/j.matchemphys.2020.122952.
- [4] E. Adamczyk and V. Pralong, " $\text{Na}_2\text{Mn}_3\text{O}_7$ : A Suitable Electrode Material for Na-Ion Batteries?," *Chem. Mater.*, vol. 29, no. 11, pp. 4645–4648, 2017, doi: 10.1021/acs.chemmater.7b01390.
- [5] P. Zheng *et al.*, "A High-Performance Primary Nanosheet Heterojunction Cathode Composed of  $\text{Na}_{0.44}\text{MnO}_2$  Tunnels and Layered  $\text{Na}_2\text{Mn}_3\text{O}_7$  for Na-Ion Batteries," *ChemSusChem*, vol. 13, no. 7, pp. 1793–1799, 2020, doi: 10.1002/cssc.201903543.
- [6] Y. Fang, X. Y. Yu, and X. W. (David) Lou, "Nanostructured Electrode Materials for Advanced Sodium-Ion Batteries," *Matter*, vol. 1, no. 1, pp. 90–114, 2019, doi: 10.1016/j.matt.2019.05.007.
- [7] Y. Liu, C. Sun, Y. Li, H. Jin, and Y. Zhao, "Recent progress of Mn-based NASICON-type sodium ion cathodes," *Energy Storage Mater.*, vol. 57, pp. 69–80, Mar. 2023, doi: 10.1016/j.ensm.2023.02.005.
- [8] K. Kubota, M. Dahbi, T. Hosaka, S. Kumakura, and S. Komaba, "Towards K-Ion and Na-Ion Batteries as 'Beyond Li-Ion,'" *Chem. Rec.*, vol. 18, no. 4, pp. 459–479, Apr. 2018, doi: 10.1002/tcr.201700057.
- [9] M. Jiang *et al.*, "Nickel-cobalt layered double hydroxide cathode materials with excellent cycle stability for nickel-metal hydride batteries," *J. Alloys Compd.*, vol. 941, p. 168980, Apr. 2023, doi: 10.1016/j.jallcom.2023.168980.
- [10] Q. Shao *et al.*, "A Redox Couple Strategy Enables Long-Cycling Li- and Mn-Rich Layered Oxide Cathodes by Suppressing Oxygen Release," *Adv. Mater.*, vol. 34, no. 14, Apr. 2022, doi: 10.1002/adma.202108543.
- [11] Y. Huang *et al.*, "Manganese (II) chloride leads to dopaminergic neurotoxicity by promoting mitophagy through BNIP3-mediated oxidative stress in SH-SY5Y cells," *Cell. Mol. Biol. Lett.*, vol. 26, no. 1, p. 23, Dec. 2021, doi: 10.1186/s11658-021-00267-8.
- [12] B. Song *et al.*, "Understanding the Low-Voltage Hysteresis of Anionic Redox in  $\text{Na}_2\text{Mn}_3\text{O}_7$ ," *Chem. Mater.*, vol. 31, no. 10, pp. 3756–3765, May 2019, doi: 10.1021/acs.chemmater.9b00772.

- [13] Y. Wang *et al.*, “The novel P3-type layered  $\text{Na}_{0.65}\text{Mn}_{0.75}\text{Ni}_{0.25}\text{O}_2$  oxides doped by non-metallic elements for high performance sodium-ion batteries,” *Chem. Eng. J.*, vol. 360, pp. 139–147, Mar. 2019, doi: 10.1016/j.cej.2018.11.214.
- [14] N. Kızıldaş-Yavuz *et al.*, “Synthesis, structural, magnetic and electrochemical properties of  $\text{LiNi}_{1/3}\text{Mn}_{1/3}\text{Co}_{1/3}\text{O}_2$  prepared by a sol–gel method using table sugar as chelating agent,” *Electrochim. Acta*, vol. 113, pp. 313–321, Dec. 2013, doi: 10.1016/j.electacta.2013.09.065.
- [15] N. Priyadharsini, P. Rupa Kasturi, A. Shanmugavani, S. Surendran, S. Shanmugapriya, and R. Kalai Selvan, “Effect of chelating agent on the sol-gel thermolysis synthesis of  $\text{LiNiPO}_4$  and its electrochemical properties for hybrid capacitors,” *J. Phys. Chem. Solids*, vol. 119, pp. 183–192, Aug. 2018, doi: 10.1016/j.jpcs.2018.03.004.
- [16] R. Septawendar, A. Nuruddin, S. Sutardi, E. Maryani, L. A. T. W. Asri, and B. S. Purwasasmita, “Low-temperature metastable tetragonal zirconia nanoparticles (NpMTZ) synthesized from local zircon by a modified sodium carbonate sintering method,” *J. Aust. Ceram. Soc.*, vol. 54, no. 4, pp. 643–654, Dec. 2018, doi: 10.1007/s41779-018-0193-4.
- [17] I. Ismail, N. Osman, and A. M. M. Jani, “ $\text{La}_{0.6}\text{Sr}_{0.4}\text{Co}_{0.2}\text{Fe}_{0.8}\text{O}_{3-\delta}$  powder: a simple microstructure modification strategy for enhanced cathode electrochemical performance,” *J. Sol-Gel Sci. Technol.*, vol. 94, no. 2, pp. 435–447, May 2020, doi: 10.1007/s10971-020-05231-0.